

LONG-TERM PASSIVE COOLING FOR THE ACCELERATOR PRODUCTION OF TRITIUM

Ju-Chuan Lin
Los Alamos National Laboratory
P.O. Box 1336
Los Alamos, New Mexico 87545
(505) 667-0679

Donald A. Siebe
Los Alamos National Laboratory
P.O. Box 1336
Los Alamos, New Mexico 87545
(505) 665-0533

Kemal O. Pasamehmetoglu
Los Alamos National Laboratory
P.O. Box 1336
Los Alamos, New Mexico 87545
(505) 667-8893

John N. Edwards
Los Alamos National Laboratory
P.O. Box 1336
Los Alamos, New Mexico 87545
(505) 667-7552

ABSTRACT

A cavity flooding system has been designed to provide long-term cooling for the Accelerator Production of Tritium target/blanket system during an internal or external large-break loss-of-coolant accident. The cavity is flooded with water from the spent module storage pool. If no active cooling systems are available, then the water in the cavity will be heated gradually to a saturation temperature corresponding to the cavity pressure and then will be boiled off very slowly. An analysis was performed, and the results show that the natural circulation flow in the cavity during the boil-off is large enough to cool the target and blanket.

I. INTRODUCTION

A cavity flooding system has been designed to provide long-term cooling for the Accelerator Production of Tritium (APT) target/blanket system during an internal or external large-break loss-of-coolant accident. The actual design for the cavity flooding system is given in the System Design Description (SDD) report (Ref. 1). Figure 1 shows the schematic diagram for the cavity flood system. The cavity is flooded with water from the spent module storage pool. If no active cooling systems are available, the water in the cavity will be heated gradually to a saturation temperature corresponding to the cavity pressure and then boiled off very slowly. The objective of this paper is to analyze the thermal-hydraulic behavior in the cavity vessel after flooding. The Transient Reactor Analysis Code (TRAC), a computer code (Ref. 2) developed by Los Alamos National Laboratory, was used to perform the analysis.

II. TRAC CODE VERSION

The most recent version of TRAC-PF1/MOD2, Version 29 plus, was used to perform the analysis. The version is similar to the earlier version of TRAC-PF1/MOD2, except that error corrections are included. For steady-state calculations, the code uses the underrelaxation method to calculate the interfacial drag and heat/mass transfer. In general, the code runs with a larger timestep using the steady-state option. For the long-term cooling analysis, the transient is in a quasi-steady mode. The underrelaxation scheme should be applicable to this situation. Therefore, we modified the code by invoking the underrelaxation scheme to speed up the calculation.

III. DESCRIPTION OF TRAC INPUT MODEL

Figure 1 shows the schematic of the APT cavity flood system. For the long-term cooling analysis, we modeled only the cavity vessel and the vent system because the cavity flooding phase already was over and

DISCLAIMER

This report was prepared as an account of work sponsored by an agency of the United States Government. Neither the United States Government nor any agency thereof, nor any of their employees, make any warranty, express or implied, or assumes any legal liability or responsibility for the accuracy, completeness, or usefulness of any information, apparatus, product, or process disclosed, or represents that its use would not infringe privately owned rights. Reference herein to any specific commercial product, process, or service by trade name, trademark, manufacturer, or otherwise does not necessarily constitute or imply its endorsement, recommendation, or favoring by the United States Government or any agency thereof. The views and opinions of authors expressed herein do not necessarily state or reflect those of the United States Government or any agency thereof.

DISCLAIMER

Portions of this document may be illegible in electronic image products. Images are produced from the best available original document.

the vapor generated in the cavity vessel would exit through the vent system. The lateral power distribution from the beam centerline was almost symmetrical. Therefore, we modeled only half of the cavity vessel.

A. Hydraulic Model

The vent system was modeled with a one-dimensional (1D) VALVE component. The cavity vessel was modeled with a three-dimensional (3D) VESSEL component with Cartesian geometry, as shown in Fig. 2. The Cartesian geometry was selected because the blankets and most of shield blocks are designed in a rectangular geometry. The vessel consists of eight axial levels: four lateral meshes in the x direction and five lateral meshes in the y direction. The outer cells were blocked off to map the cylindrical wall of the cavity vessel. The blocked flow area and the volume occupied by the target ladders, blankets, and shield blocks in levels 1 to 6 were modeled. The upper header of the cavity vessel was modeled as an open region in levels 7 and 8. The flow area and volume occupied by the pipes in the upper header were not modeled.

The annular downcomer region was modeled by cutting a half-cylinder annular region from levels 1 to 6, as shown in Fig. 2. The window region was modeled by opening a channel on the surface formed by mesh 1 in the y direction and mesh 4 in the x direction from levels 3 to 5. The target chamber was modeled in the region formed by meshes 2 and 3 in the y direction and mesh 4 in the x direction from levels 3 to 5. The target volume was subtracted from the total target chamber volume. Also, the flow area blocked by the target chamber was subtracted from the total flow area of each surface.

The space between the concrete structure and the cavity vessel was modeled with 11 pipes by preserving the total volume of the space. The heat loss from the cavity vessel wall to the space was modeled with 11 heat structures.

B. Heat Structure Model

Figure 3 shows the unit cell geometry for the lateral row-1 blanket. The unit cell geometry for the blankets of other modules is similar to the lateral row-1 blanket. The unit cell was modeled as a hollow cylinder with liquid flowing in the center channel, as shown in Fig. 4. In the model, the total volume of materials of the unit cell was preserved because for the long-term cooling analysis, it is far more important to model the total heat capacity of the unit cell correctly than the temperature distribution. Also, the surface in contact with the liquid in the cavity vessel was preserved such that the heat-transfer area to the cavity fluid could be calculated correctly. However, the thickness and the surface area of the materials were not preserved.

The mesh boundaries of the hydro model were almost in line with the module boundaries. A lumping methodology was developed to combine different rows and the decoupler of a blanket. For the front lower blanket of module 1, we combined the decoupler with rows 1 through 5. The total aluminum volume of the decoupler was added to the aluminum volume of the outer ring because the decoupler tubes did not contact the water in the cavity. A similar lumping methodology was applied to the back lower blanket, the upper front blanket, the module-2 downstream blanket, the upstream upper blanket, and the upstream lower blanket.

The rung of the target ladders consists of a center rod and concentric tungsten rings clad with Inconel and a stainless-steel outside shell. We lumped the rungs a cylinder pipe with a wall consisting of tungsten, Inconel, and stainless steel. The total volume of each material was preserved.

C. Power

The power distribution for the blankets is given in Ref. 3. The power for a lumped heat structure was calculated by adding the power of each blanket of the lumped heat structure. Reference 4 gives the power decay fraction for all of the blankets. An average power decay curve, which is the total power times the decay power fraction for each blanket divided by the sum of the total power, was used for this analysis.

The power distribution for the target and the power decay fraction for each ladder are given in Refs. 3 and 4, respectively. In this analysis, the decay power fraction was increased by 20% and the normal operating power for the hot ladder was multiplied by a factor of 1.2 to account for uncertainties. A power decay curve calculated with the same method as the blanket was used for this analysis.

IV. INITIAL AND BOUNDARY CONDITIONS

A lumped heat conduction modeling was performed. The results showed that it takes approximately 11 days to heat the water in the cavity vessel to saturation temperature corresponding to the cavity pressure. It would take many hours of computational time for the system to heat up gradually. Therefore, we set the water temperature to the saturation temperature initially. The boundary conditions for the vent valve are assumed to be at atmospheric pressure (1.01325×10^5 Pa) and ambient temperature (300 K). The cavity vessel was filled to 1.58 m above the bottom of level 8. This equilibrium level between the flood pool and the cavity vessel was calculated in Ref. 4, which is approximately 14 m above the bottom of the cavity vessel.

V. RESULTS

In one calculation, we assumed that the space above the top of the liquid level was filled with air. However, the results were very oscillatory and nonphysical due to the interfacial heat/mass transfer problems with noncondensable gas at low pressure. For this analysis, we assumed that the space is filled with steam.

Figure 5 shows the liquid velocities from levels 3 to 7 of the first sector. The liquid velocities oscillate during the first 2000 s and then decrease gradually. At approximately 6000 s, the velocities decrease rapidly and then decrease very slowly. The sudden reduction in velocity occurs when the residual heat is too low to produce vapor in the high power regions, as shown from Figs. 6 through 10. Before approximately 6000 s, the circulation flow is induced by the boiling. After 6000 s, the circulation flow transits into a natural circulation mode.

Figures 6 through 10 show the void fractions for cells with high-power modules. Voids are generated in level 7 during the first 6000 s. After 6000 s, voids are collapsed because the residual heat is too low to produce vapor in the high-power regions. This implies that the natural-circulation flow keeps the target and blankets cool after 6000 s.

Figures 11 to 14 show the mass flows for each cell at axial level 6, where the top shielding blocks are located. Because we are interested in the quasi-steady-state results, the time of those plots begins from 10,000 s. After 30,000 s, the liquid flows almost reach quasi-steady state. The liquid flows for the annular downcomer are downward (negative value), except for the cell for the back module. Similarly, the flows for the shielding block and low-power modules are downward. However, the liquid flows for the high-power modules are upward (positive value). This implies that flow enters from the annular downcomer, the shielding block, and the low-power regions and exits from the high-power module regions. Figure 15 shows a mass balance in the axial (z) direction for the in and out flows at level 6. The maximum difference is approximately -0.01 kg/s.

Figure 16 shows the total mass flow for the annular downcomer. The mass flow reaches a steady down flow of approximately -47 kg/s at 20 hours.

VI. CONCLUSIONS

A TRAC model was developed to study long-term passive cooling for the APT. The results show that a natural-circulation flow pattern has been established where flow is down the annular region between the outermost shielding blocks and the vessel, to the target cavity region, through the window opening, up from

the target cavity region to the cavity upper header, and through the gaps between the upper shielding blocks. The natural-circulation flow keeps the target and blankets cool.

REFERENCES

1. System Design Description for Target Heat Removal System, DOE APT Project, Technical Project Office report T21-G-SDD-X-001, Revision 0 (September 1997).
2. Safety Code Development Group, TRAC-PF1/MOD2 Theory Manual, Los Alamos National Laboratory report LA-12031-M, Vol. I, NUREG/CR-5673 (July 1993).
3. H. R. Trelue, Decay Heat and Gamma Redistribution Calculation, Los Alamos National Laboratory TSA-10 calc-note CN-APT/TSA10-018 (July 2000).
4. D. Siebe, "Cavity Vessel Fill and Vent Calculations," Los Alamos National Laboratory calc-note CN-APT/TSA10-028 (August 2000).

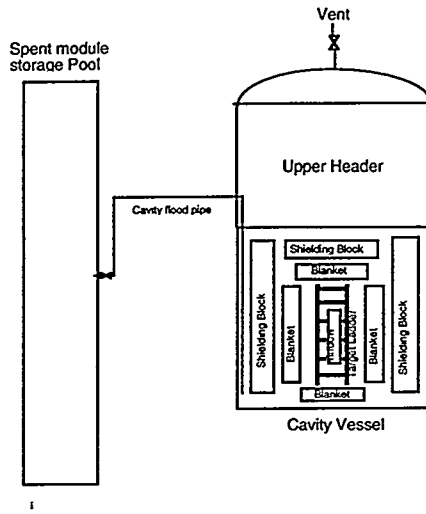


Fig. 1. Schematic diagram for the cavity flood system.

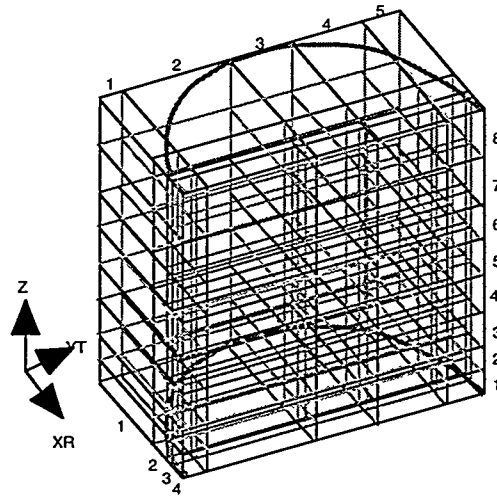


Fig. 2. Cavity vessel nodalization diagram.

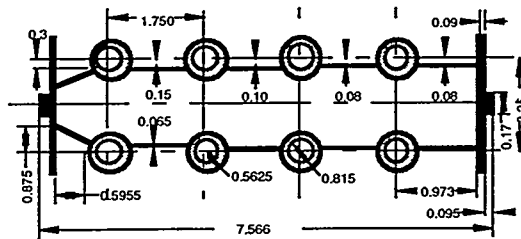


Fig. 3. Unit cell geometry for the lateral Row-1 blanket.

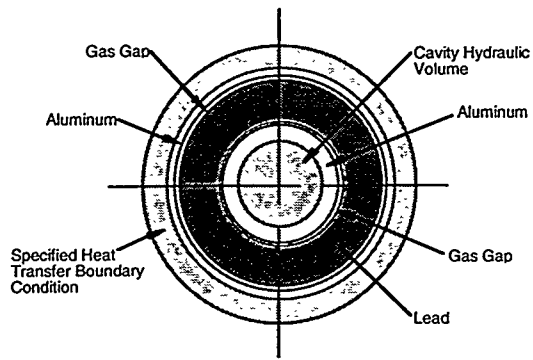


Fig. 4. A hollow cylinder HEAT STRUCTURE model for a unit cell.

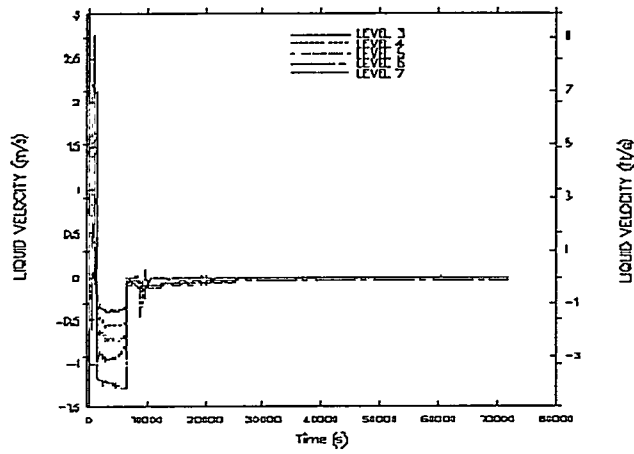


Fig. 5. Axial liquid velocities for the cells ($x = 1, y = 1, z = 3$ to 7).

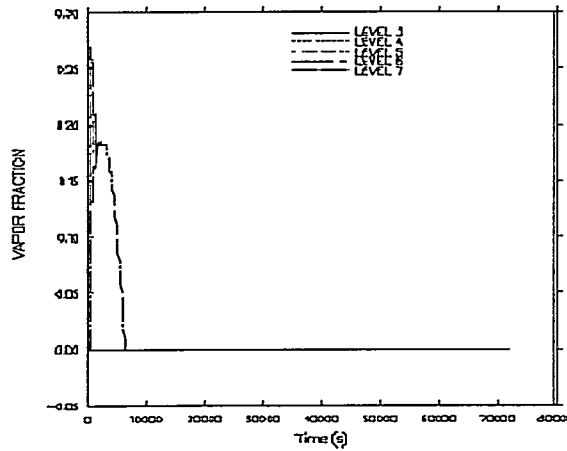


Fig. 6. Void fractions for the cells ($x = 4, y = 1, z = 3$ to 7).

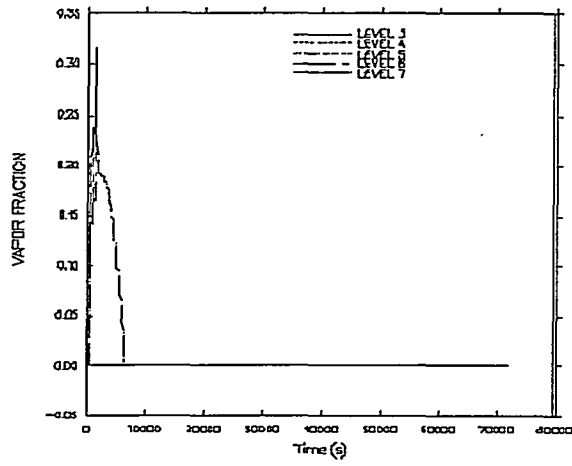


Fig. 7. Void fractions for the cells ($x = 4, y = 2, z = 3$ to 7).

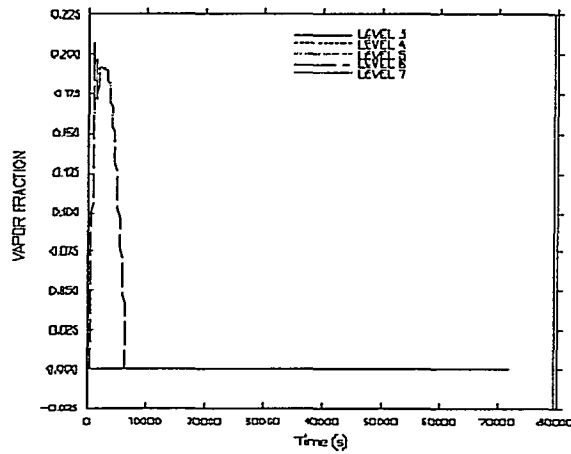


Fig. 8. Void fractions for the cells ($x = 4, y = 3, z = 3$ to 7).

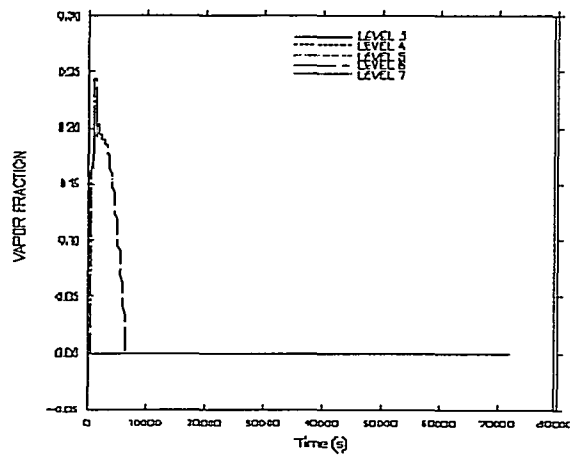


Fig. 9. Void fractions for the cells ($x = 4, y = 4, z = 3$ to 7).

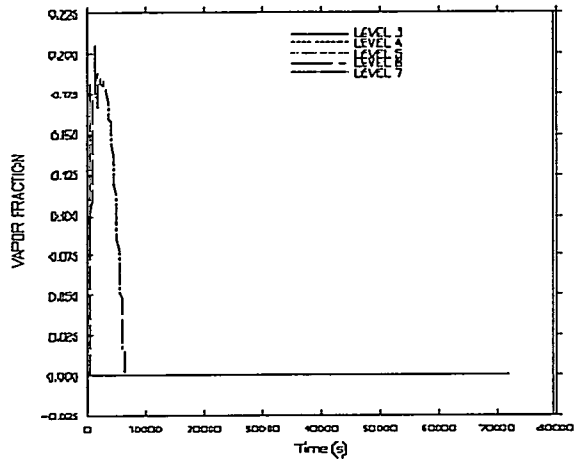


Fig. 10. Void fractions for the cells ($x = 4, y = 5, z = 3$ to 7).

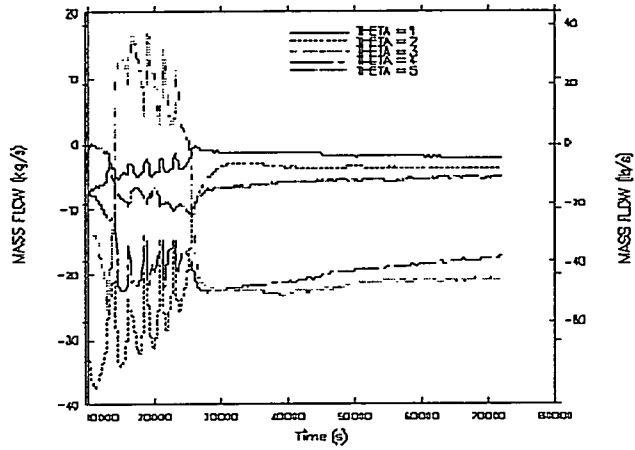


Fig. 11. Axial liquid mass flows for the cells ($x = 1, y = 1$ to $5, z = 6$).

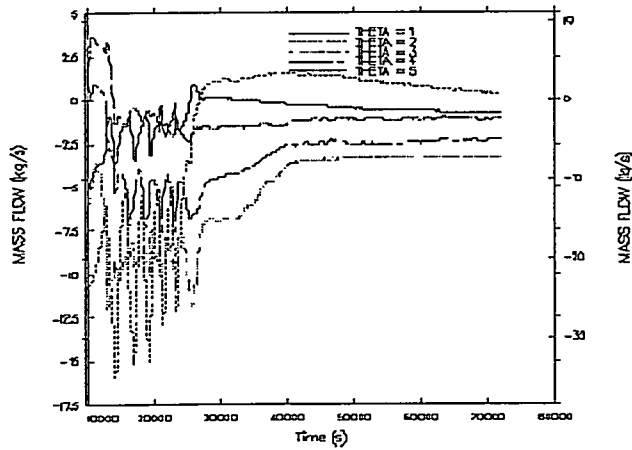


Fig. 12. Axial liquid mass flows for the cells ($x = 2, y = 1$ to $5, z = 6$).

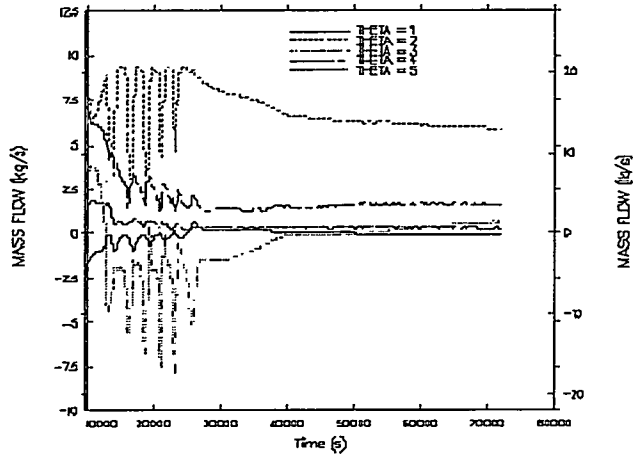


Fig. 13. Axial liquid mass flows for the cells ($x = 3, y = 1$ to $5, z = 6$).

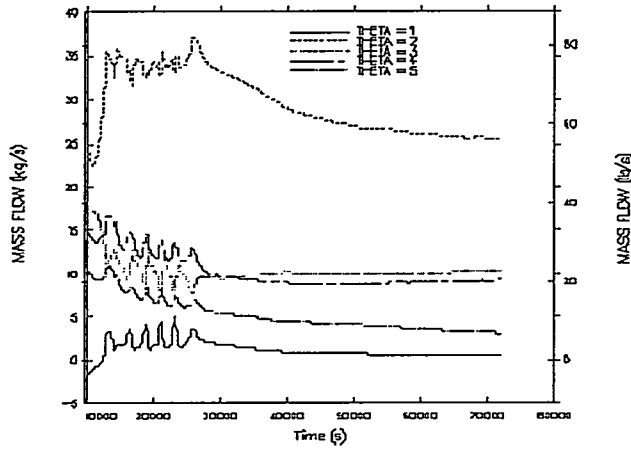


Fig. 14. Axial liquid mass flows for the cells ($x = 4, y = 1$ to $5, z = 6$).

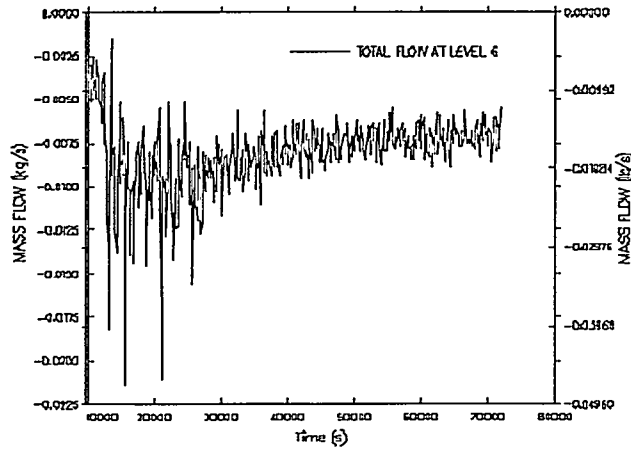


Fig. 15. Total axial liquid mass flow at level 6 ($z = 6$).

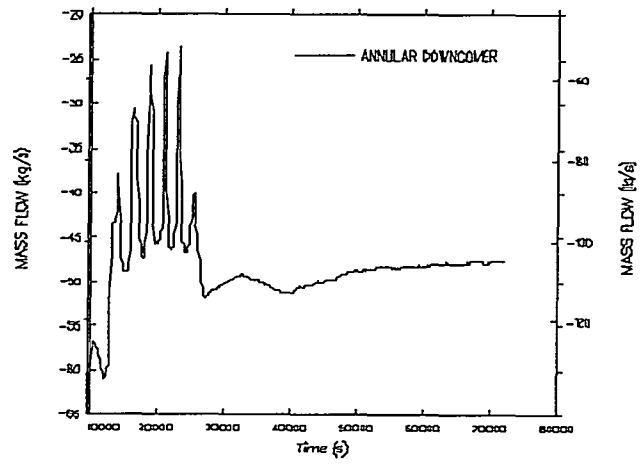


Fig. 16. Total axial liquid mass flow in the annular downcomer region at level 6.